

## Potential use of moroccan fly ash as low cost adsorbent for the removal of two anionic dyes (indigo carmine and acid orange)

M. EL Alouani, S. Alehyen, M. EL Achouri\*, M. Taibi

Mohammed V University in Rabat,

Laboratoire de Physico-chimie des Matériaux Inorganiques et Organiques (LPCMIO), Ecole Normale Supérieure BP : 5118.  
Takaddoum -Rabat-Morocco

Received 19 Apr 2016,  
Revised 25 Apr 2017,  
Accepted 29 Apr 2017

### Keywords

- ✓ Fly ash
- ✓ Adsorption model
- ✓ Kinetics
- ✓ Thermodynamics
- ✓ Anionic dye.

[achmedens@yahoo.fr](mailto:achmedens@yahoo.fr)

[ma.elalouani@gmail.com](mailto:ma.elalouani@gmail.com)

### Abstract

The aim of this study is the valorization of fly ash, by-products of the JorfLasfar power plant in removing organic anionic dyes pollutants (indigo carmine and acid orange 52). The effects of contact time, pH and initial concentrations of the dyes, fly ash adsorbent dose and temperature on the removal of anionic dyes by fly ash were studied in batch mode. The removal of the two dyes (indigo carmine and acid orange 52) increases with the increase of contact time and dyes initial concentrations. Thus, the equilibrium adsorption capacity ( $q_e$ ) was increased with increasing contact time and initial dye concentration. The adsorption capacity of fly ash is independent of pH over the pH range 2-14. The results show that fly ash is an excellent adsorbent matrix. Indeed, for a fly ash concentration of 2.5 g/L, the dye removal percentages were 100% for indigo carmine dye and 90% for the Acid Orange dye. Three kinetic models, pseudo first order, pseudo second order and the intra particle diffusion models were selected to study the adsorption process. The kinetic parameters, the rate constants, the equilibrium adsorption capacities and the correlation coefficients for each kinetic model were calculated and discussed. The best results were achieved with the pseudo second-order kinetic model. Experimental data were analyzed using the equations of Langmuir and Freundlich isotherm models. The best fit was obtained by the Langmuir isotherm model. The thermodynamic parameters, such as  $\Delta H^\circ$ ,  $\Delta S^\circ$  and  $\Delta G^\circ$  were also experimentally determined. The adsorption kinetic mechanisms, and the substrate capacities are further discussed while correlated with the surface structure (XRD), composition (FX, FTIR), and morphology (SEM). The results indicate that the fly ash can be used as an efficient and low cost adsorbent for the removal of textile dyes from effluents. This work can help in designing low cost adsorption columns for treating effluent water in industries or other adsorption processes.

### 1. Introduction

The presence of organic dyes in aqueous environments can cause harmful effects on human beings and aquatic life as a result of their toxicity. Moreover, discharging effluents containing organic dyes into receiving water results in preventing light diffusion into aqueous phase [1-3].

This massive influx of untreated organic chemicals into the waterways not only introduces aesthetic concerns, but far more importantly it promotes eutrophication and adversely affects the environmental health of the region. It also represents an increasing environmental danger due to their refractory carcinogenic nature [4].

Various chemical, physical and biological processes have been used to remove dyes from industrial effluents [5]. Some of these conventional waste treatment technologies are: trickling filter, activated sludge chemical coagulation, flocculation, oxidation or ozonation, membrane separation, photodegradation and adsorption processes [6-8].

All these methods are significantly different in terms of color removal, operation and financial cost [9,10]. The removal of the dyes in aqueous solutions by adsorption on different solid materials, in particular on activated carbon, has been the subject of many studies [11-13].

Activated coal is the most popular adsorbent, which is able to adsorb many dyes with a high adsorption capacity [14-17]. It is very expensive and the cost of regeneration is high because desorption of the dye molecules is not easily achieved [18].

Also, activated coal is the most widely used adsorbent due to its excellent adsorption capability. However, its use is often limited due to high cost, making this method unfavorable for the needs of developing countries like Morocco; in such cases, the use of low-cost adsorbents, such as clay minerals [19], natural phosphate [20], kaolinite [21], silica [22] and Fly ash [23-27], is a promising alternative due to their relative abundance and their low commercial value. Attempts have been made by various workers to use fly ash as low-cost materials and it remains a potential low-cost adsorbent for the future. Fly ash is a waste substance from thermal power plants that is found in abundance. Morocco generates a lot of coal fly ash each year in the three power stations (JorfLasfar, Jerrada, Mohammedia). Fly ash produced in large scale causes major disposal problems.

For the present study, a batch-contact-time method was used to assess the potentiality of fly ash as a low-cost adsorbent for the removal of anionic dyes in aqueous solution. Adsorption studies were carried out under various parameters such as pH, contact time, initial dye concentration and temperature. Experimental data were performed for isotherm models such as Langmuir and Freundlich. The adsorption rates were determined quantitatively and simulated by the Langmuir, the pseudo-first-order and second-order models, and then adsorption mechanism was analyzed using intra-particle diffusion. Furthermore, thermodynamic activation parameters were also determined.

## 2. Materials and Methods

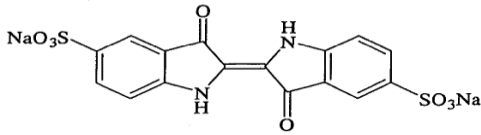
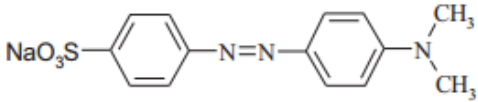
### 2.1. Adsorbent material

Coal fly ash, a solid waste obtained from combustion of coal. Chemical constituents of fly ash mainly depend on the chemical composition of the coal [28]. The fly ash used in this study was from thermal coal plant of JorfLasfar in Morocco. The sample was sieved through sieve to obtain lower fractions (< 200 μm). The fly ash is characterized by many physico-chemical methods: The chemical composition of adsorbent was obtained by X-ray fluorescence using a spectrometer dispersion wavelength - Type Axios. X-ray diffraction (XRD) patterns of the samples were obtained using aXpert Pro model diffractometer equipped with a monochromatic source operating Cu-Kα (1.54060 Å). The Fourier transform infrared (FTIR) spectra of the samples were recorded by the KBr pellet technique on a VERTEX 70 FTIR spectrometer, in the spectral range of 4000–400 cm<sup>-1</sup> with 4 cm<sup>-1</sup> resolution. Image of fly ash were characterized by a detector type (SUTW-Sapphire, Resolution: 230.89, Lsec: 111). The morphology and structure of the material were characterized by a scanning electron microscope (SEM) analysis and Transmission electron microscopy (TEM).

### 2.2. Dyes

The indigo carmine and acid orange 52 were used to determine the adsorption performance of the fly ash. The chemical formula and some other specific characteristics of these dyes are summarized in Table 1.

**Table 1:** Physicochemical characteristics of used dyes.

Name	$\lambda_{\max}$ (nm)	Molar mass (g/mol)	Molecular structure
<b>Indigo Carmine (CI)</b> (Anionic)	<b>610</b>	<b>466,36</b>	
<b>Acid Orange 52 (AO 52)</b> (Anionic)	<b>464</b>	<b>327,33</b>	

### 2.3. Adsorption experiments

The effects of initial dye concentration, contact time, temperature and pH on the adsorption of dyes on the fly ash were studied. After each completed absorption test, the sample was separated by specific filters. The supernatant were analyzed for residual dye concentration by JASCO V-630 UV / VIS spectrophotometer. The adsorbed quantity was calculated using the following equations:

$$Q_e = \frac{(C_0 - C_e)}{m} V \quad (1)$$

Where  $C_0$  and  $C_e$  are the initial and the equilibrium concentration of dye (mg/L), respectively,  $m$  is the mass of adsorbent (g) and  $V$  (L) is the solution volume.

The dye removal percentage can be calculated as follows:

$$\% \text{ removal} = \frac{(C_0 - C_e)}{C_0} \times 100 \quad (2)$$

#### 2.3.1. Effect of adsorbent mass

In beaker containing 100 mL of the colored solution at 14 mg/L of  $23 \pm 2^\circ\text{C}$  and pH 6.4, we introduced growing masses of fly ash from 0.2 to 2.5g. The resulting mixture was then stirred (400 rpm) for 1hour, the resulting supernatants were analyzed for to calculate the residual concentration and % removal of dyes.

#### 2.3.2. Effect of pH

The solution pH is an important parameter in controlling the adsorption capacity of the ionic organic materials on the substrate [29]. It affects not only the adsorbent surface charge, but also the dyes ionization. Batch pH studies were conducted by shaking 100mL of each dye solution with 1g of the fly ash for 1hour in pH range value from 2 to 14. The solution pH was adjusted with HCl or NaOH solution.

#### 2.3.3. Adsorption isotherms

The adsorption isotherms are often exploited to determine the maximum capacities of fixing anionic dyes and for the identification of the adsorption type. The results processed according to mathematical models of Langmuir and Freundlich.

#### Langmuir Model

The first most commonly used model is the Langmuir one [30]. The initial assumptions are that the solid adsorbent has a limited adsorption capacity ( $q_m$ ), all active sites are identical, they can be complexed one solute molecule (monolayer adsorption) and that there are no interactions between the adsorbed molecules [31]. The linearized equation is given as follows:

$$\frac{C_e}{Q_e} = \frac{1}{K_L Q_m} + \frac{C_e}{Q_m} \quad (3)$$

Where  $Q_e$  (mg/g) is the adsorbed amount at equilibrium,  $C_e$  is the equilibrium dye concentration (mg/L),  $K_L$  is Langmuir equilibrium constant (L/mg) and  $Q_m$  the maximum adsorption capacity (mg/g).

The shape of the Langmuir isotherm is indicated by separation factor or equilibrium parameter  $R_L$  [32], defined by:

$$R_L = \frac{1}{1 + K_L C_0} \quad (4)$$

Where  $C_0$  (mg/L) is the initial adsorbate concentration and  $K_L$  (L/mg) is the Langmuir constant related to the energy of adsorption (L.mg<sup>-1</sup>).

Valeur de $R_L$	Type isotherm
$R_L > 1$	unfavorable
$R_L = 1$	Linear
$0 < R_L < 1$	Favorable
$R_L = 0$	Irreversible

### Freundlich Model

The Freundlich isotherm can be applied to non-ideal adsorption on heterogeneous surfaces as well as multilayer sorption. A mathematical expression of the Freundlich isotherm is given by the following equations [33,34].

$$q_e = K_F C_e^{1/n} \quad (5)$$

Where  $K_F$  ( $\text{mg}^{1-1/n} \text{g}^{-1} \text{L}^{1/n}$ ) is the Freundlich constant and  $n$  ( $\text{g/L}$ ) is the heterogeneity factor. The  $K_F$  value is related to the adsorption capacity; while  $1/n$  value is related to the adsorption intensity. A linear form of this expression is:

$$\text{Log } q_e = \text{Log } K_F + \frac{1}{n} \text{Log } C_e \quad (6)$$

#### 2.3.4. Adsorption kinetics

This procedure is similar to batch equilibrium studies. The difference is that the absorbent-absorbate solution was taken at pre-defined time intervals and the concentration of the solution was measured.

Several models have been established to describe the adsorption kinetics and the rate-limiting step of the process. They include models of pseudo-first and second-order kinetic model, model intra-particle diffusion and sorption model Weber and Morris, the relationship of Adam-Bohart Thomas etc [35]. The first three are the most commonly used models to study the kinetics of adsorption of the two dyes.

#### Pseudo-first-order kinetic model

Lagergren proposed a pseudo first order kinetic model [36]:

$$\log(q_e - q_t) = \log q_e - k_1 t \quad (7)$$

Where  $q_e$  and  $q_t$  are the amounts of dye adsorbed ( $\text{mg/g}$ ) at equilibrium and at time  $t$  (min), respectively, and  $k_1$  ( $\text{min}^{-1}$ ) is the rate constant of pseudo-first-order adsorption.

#### Pseudo-second-order kinetic model

The adsorption data was analyzed in term of pseudo-second-order model, described by [37].

$$\frac{t}{q_t} = \frac{1}{k_2 q_e^2} + \frac{t}{q_e} \quad (8)$$

Where  $k_2$  ( $\text{g/mg} \cdot \text{min}$ ) is the pseudo-second-order rate constant.

#### Intraparticle diffusion process

In order to identify the scattering mechanism, kinetic results were then analyzed using the intra-particle diffusion model and then the adsorption data can be represented by the following equation [38,39].

$$q_t = k_i t^{1/2} + C \quad (9)$$

Where  $C$  is the intercept and  $k_i$  is the intraparticle diffusion rate constant ( $\text{mg/g min}^{1/2}$ ).

#### 2.3.5. Thermodynamic adsorption

Adsorption is a phenomenon that can be exothermic or endothermic depending on the adsorbent material and the nature of the adsorbed molecules [40]. Thermodynamic parameters of the adsorption process were

determined from experimental data obtained at various temperatures using the equations [41.42]. For such equilibrium reactions,  $K_d$ , the distribution constant, can be expressed as:

$$K_d = \frac{q_e}{C_e} \quad (10)$$

The Gibbs free energy is:

$$\Delta G^\circ = -RTK_d \quad (11)$$

Where R is the universal gas constant (8.314 J mol/K) and T is solution temperature in K.  $\Delta H^\circ$  is the standard enthalpy,  $\Delta G^\circ$  is the standard Gibbs and  $\Delta S^\circ$  is the standard entropy.

$$\ln K_d = \frac{\Delta S^\circ}{R} - \frac{\Delta H^\circ}{RT} \quad (12)$$

### 3. Results and Discussion

#### 3.1. Characterization of fly ash

##### 3.1.1. X-ray fluorescence analysis

The chemical composition of fly ash, as determined by X-ray fluorescence and quantified as oxides, is reported in Table 2. This composition is generally similar to that of the silico-aluminous materials. The Silicon dioxide ( $\text{SiO}_2$ ) and aluminum oxide ( $\text{Al}_2\text{O}_3$ ) constitute about 80% of the total mass ( $\text{SiO}_2 + \text{Al}_2\text{O}_3 = 82.7\%$ ) and the percentage of calcium oxide was less than 10%. The large amount of  $\text{SiO}_2$  and  $\text{Al}_2\text{O}_3$  and the low calcium oxide amount in the JorfLasfar fly ash are characteristic of low- Ca Class-F fly ash.

**Table 2:** Chemical analysis (in mass%) of fly ash

chemical composition	$\text{SiO}_2$	$\text{Al}_2\text{O}_3$	L.O.I	$\text{Fe}_2\text{O}_3$	$\text{K}_2\text{O}$	$\text{MgO}$	$\text{TiO}_2$	$\text{CaO}$	$\text{SO}_3$	$\text{Na}_2\text{O}$	$\text{P}_2\text{O}_5$	Rb
wt.%	52,5	30,2	7,12	2,94	2,08	1,23	1,03	0,822	0,787	0,719	0,203	<b>0,0694</b>
chemical composition	SrO	BaO	ZrO <sub>2</sub>	Cr <sub>2</sub> O <sub>3</sub>	Nb <sub>2</sub> O <sub>5</sub>	PbO	CuO	ZnO	NiO	I	Sum	
wt.%	<b>0,0518</b>	<b>0,0484</b>	<b>0,0382</b>	<b>0,0287</b>	<b>0,0156</b>	<b>0,0146</b>	<b>0,0137</b>	<b>0,0126</b>	<b>0,0116</b>	<b>0,0109</b>	<b>100</b>	

##### 3.1.2. X-ray diffraction analysis

The X-ray diffraction analysis enables us to identify the different mineralogical phases contained in fly ash. The results are presented in Figure 1. It was found that the fly ash consisted of crystalline minerals mullite, quartz, hematite and small amounts of calcium oxide with large characteristic peaks of quartz ( $\text{SiO}_2$ ). This result is similar to that reported for a fly ash investigated. The intensity of quartz is very strong, with mullite forming a chemically stable and dense glassy surface layer. The low calcium oxide intensity is characteristic of low- Ca Class-F CFA. This result is explained by the mineralogy of the coal used, which generally consists of crystalline silica form of quartz and clay minerals phyllosilicate group [43].

##### 3.1.3. FTIR spectra analysis

An infrared analysis was performed on fly ash. IR spectrum shown in Figure 2, show that fly ash is essentially composed of silica (an intense band at 1100 to 1000  $\text{cm}^{-1}$ ) attributed to stretching vibration of groups (Si-O) of alumina and small amounts of alkali and alkaline earth oxides, the lime in the combined state. The bands appeared in the regions of 459.21 and 795.01  $\text{cm}^{-1}$  are due to the vibration mode Si-O-Al and Si-O-Si, respectively. Which confirm the presence of mullite and quartz. On the other hand, the wide strip 3441.66  $\text{cm}^{-1}$  and 1622.70  $\text{cm}^{-1}$  are respectively assigned to the stretching vibration of  $\nu(\text{OH})$  and deformation  $\delta(\text{H}_2\text{O})$ .

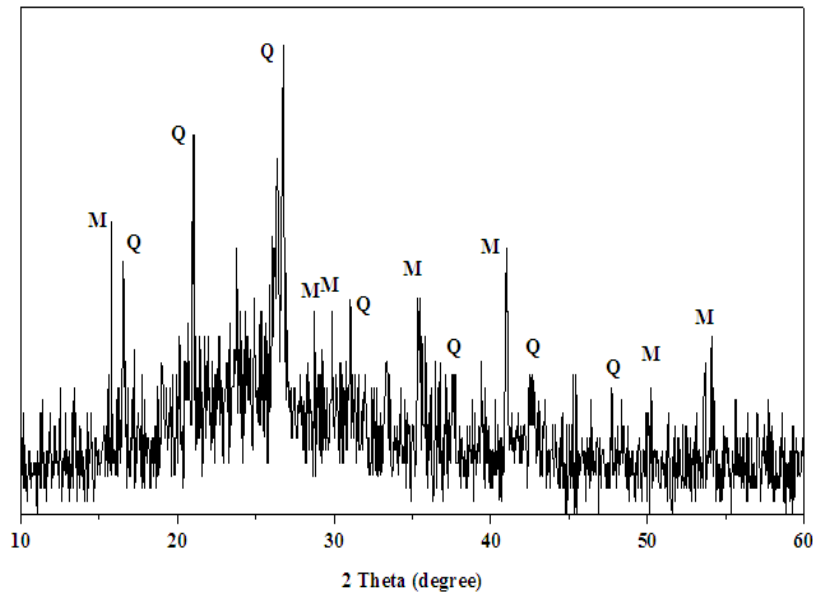


**Figure 1:** XRD patterns of fly ash (Q: Quartz; M: Mullite)

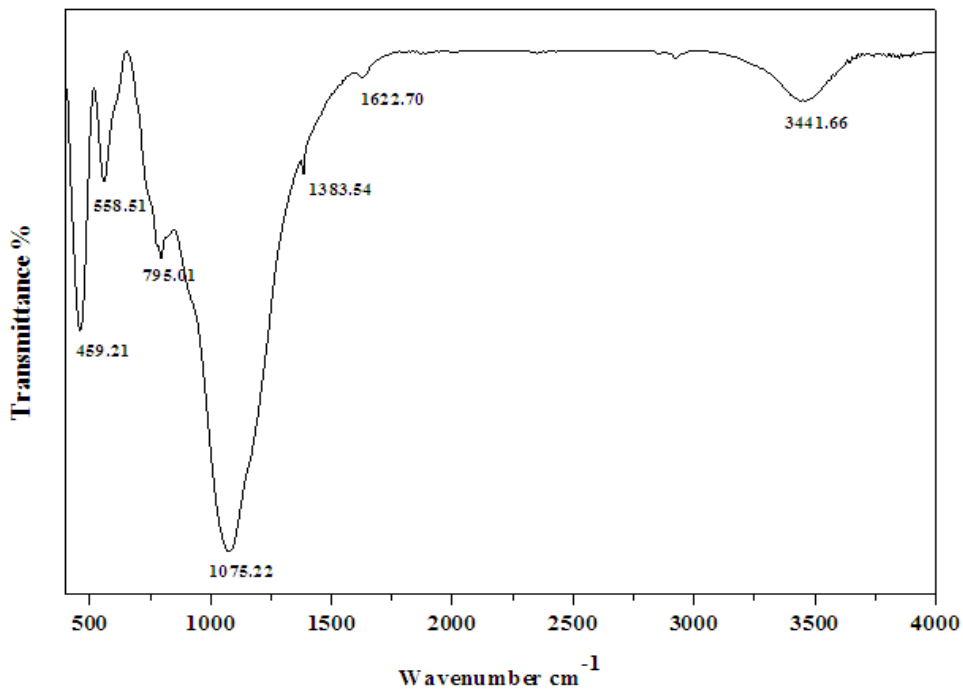


**Figure 2:** FTIR spectra of fly ash

#### 3.1.4. EDX, TEB and SEM analys

The fly ash was analyzed via EDX to quantify the surface chemical constituents. As shown in Table 3. Based on the EDX micrograph Figure 3.a.the major portion of the fly ash is composed of Si and Al compounds, which are suitable for the adsorption of various organic pollutants and inorganic from aqueous solution [44]. In addition to TEM analysis, image of fly ash is shown in Figure 3.b. As can be seen, the particle shapes of the fly ash were generally spherical and smooth surfaces. SEM is widely used to analyze the morphology of different surfaces. As can be seen in Figure 3.c, the microstructures have porous surfaces with the different sizes.

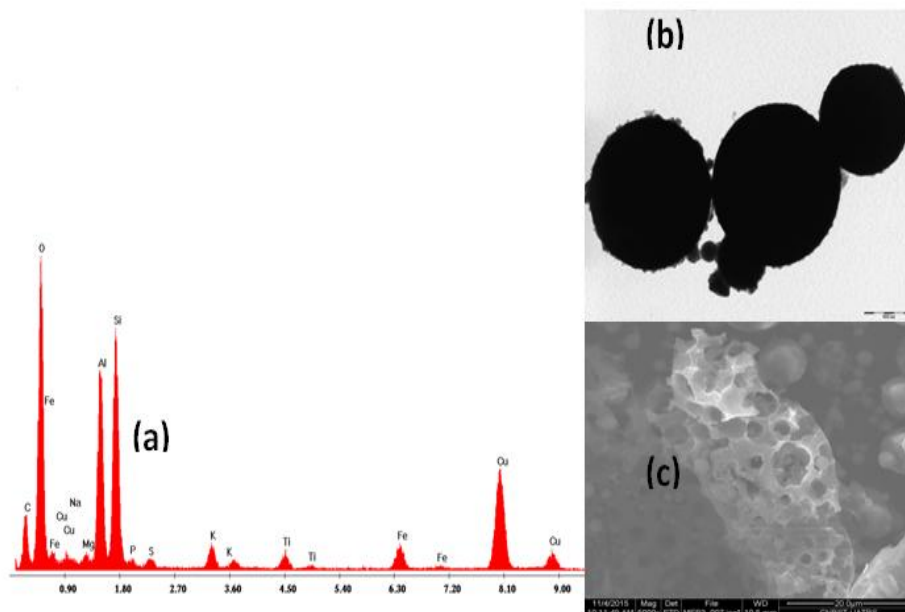


**Figure 3:** EDX micrograph (a), TEM image (b) and SEM image (c) of the fly ash

**Table 3:** The surface chemical composition of fly ash

Elements	Fly ash	
	Mass ration (wt.%)	Atomic ration (at.%)
<b>O</b>	31.9	46.6
<b>Na</b>	1.4	1.5
<b>Mg</b>	0.2	0.2
<b>Al</b>	26.7	23.2
<b>Si</b>	26	21.6
<b>P</b>	0.2	0.1
<b>S</b>	1.5	1.1
<b>K</b>	3.7	2.2
<b>Ti</b>	2.4	1.2
<b>Fe</b>	5.1	2.1
<b>Ag</b>	0.9	0.2

### 3.2. Batch adsorption studies

#### 3.2.1. Effect of adsorbent dose

The effect of adsorbent mass quantity on the removal of the dyes is shown in Figure 4. The adsorbent efficiency increased by increasing the adsorbent mass from 0.2 g to 2.5 g. 2g /L of fly ash reduces the initial concentration of dye (14mg /L) to 0.5 mg / L for the IC dye and 2.61mg/L for AO5 dye .The removal ratios are 96.4% for IC and 81.4% for AO5. The fly ash adsorption efficiency of IC dye is slightly higher than that of AO5 dye. We conclude that the extra increase in the amount of the adsorbent has a greater affinity for anionic dyesremoval and the number of sorption sites available increases by increasing the amount of adsorbent. The fly ash adsorption efficiency of anionic dyes is excellent.



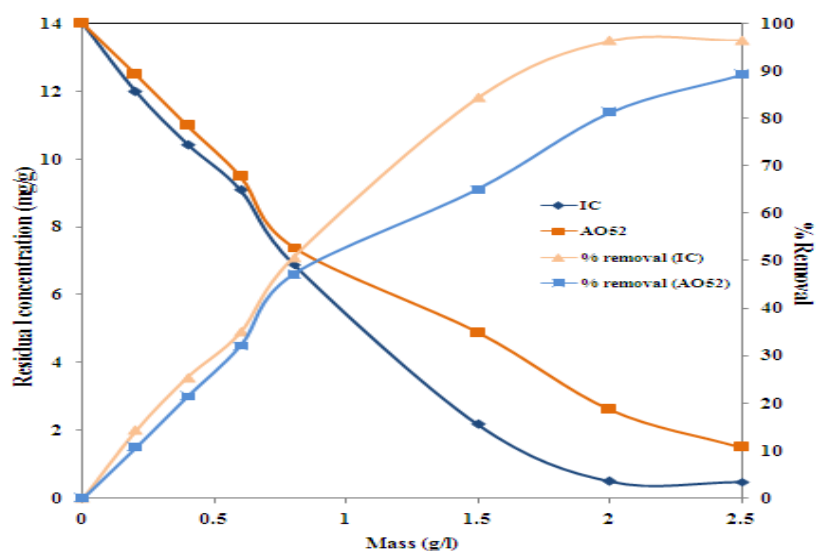


**Figure 4:** Residual concentration and % removal of indigo carmine and acid orange 52 depending on the mass of the adsorbent ( $C_0 = 14 \text{ mg/L}$ ,  $\text{pH} = 6.4$ ; Agitation = 400 rpm; Contact time = 1 hour,  $T = 23 \pm 2^\circ\text{C}$ ).

### 3.2.2. Effect of pH

In order to evaluate the influence of pH on the adsorption, we conducted a series of experiments using solutions of both anionic dyes with 14 mg/L of concentration. The dyes solutions were mixed with fly ash concentration of 1g/L, and the mixture pH were adjusted to the values ranging between 2 and 14 with HCl or NaOH. The changes observed in the adsorption of indigo carmine and Acid Orange 52 with fly ash are shown in Figure 5. The figures indicate that the amount adsorbed increased as the pH between the range 2 to 4 and from 8 to 14. Remained constant in the pH interval between 4 to 8. The adsorption is high in acid and basic medium. The change of pH affects the adsorption process through the dissociation of functional groups on the active site of the adsorbent. This subsequently leads to the shift in reaction kinetics and equilibrium characteristics of the adsorption process [45]. In this work, all removal tests on fly ash were affected at normal pH of the solution (without correction) to avoid a possible effect of pH.

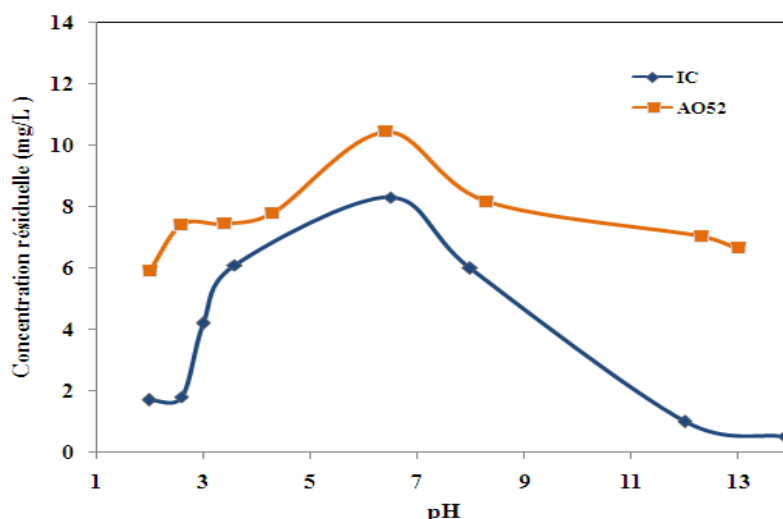


**Figure 5:** Influence of pH on the adsorption of indigo carmine and acid orange 52 of fly ash ( $C_0 = 14 \text{ mg/L}$ ,  $m=1\text{g/L}$ ; Agitation = 400 rpm ; Contact time = 1 hour,  $T = 23 \pm 2^\circ\text{C}$ ).

### 3.2.3. Adsorption isotherms

The study of the isotherm adsorption equilibrium is fundamental to determining the capacity and nature of the adsorption of both studied dyes. The results obtained by using the templates are shown respectively in Figure 6 and 7.



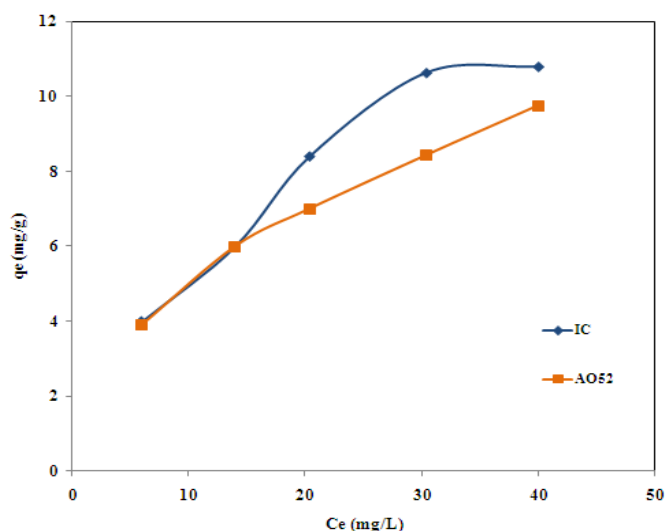


**Figure 6:** Equilibrium isotherms of IC and AO25 on fly ash ( $m=1\text{g/L}$ ; Agitation = 400 rpm;  $\text{pH}=6,4$ ; Contact time = 1 hour,  $T = 23 \pm 2^\circ\text{C}$ ).

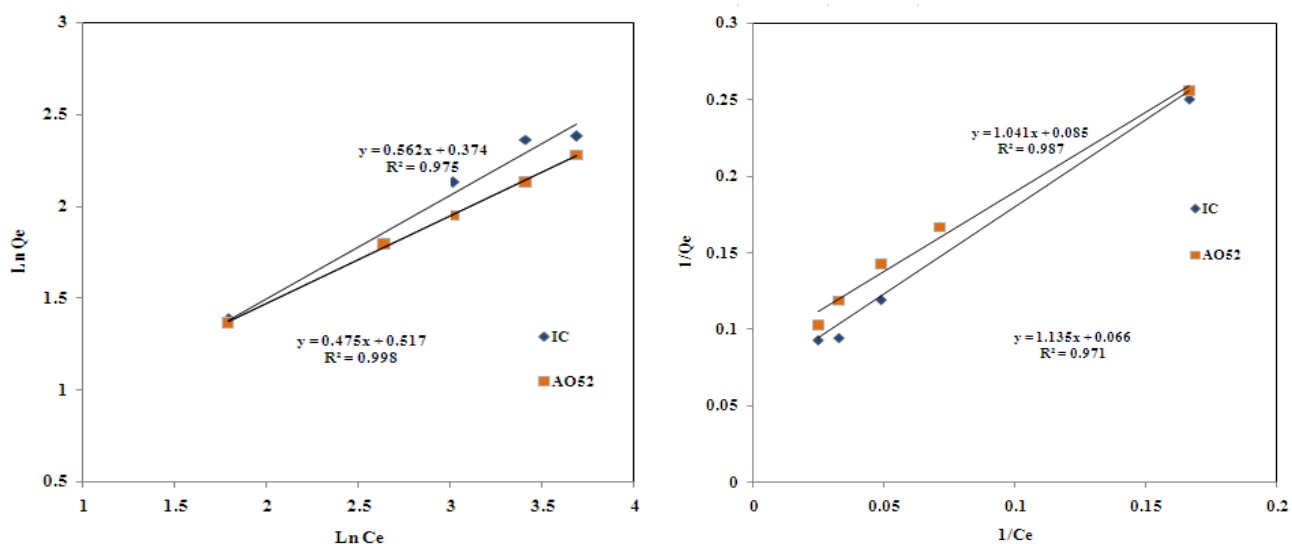


**Figure 7:** Linearization of the Langmuir and Freundlich equation for adsorption IC and AO52 on fly ash.

The values of constants Langmuir and Freundlich calculated by linear regression from the curves were summarized in Table 4.

**Table 4:** isotherm models constants for the dyes adsorption onto fly ash.

Fly ash			
Isotherm	Parameters	Indigo Carmine(IC)	Acid Orange 52 (AO52)
Langmuir	$Q_{\max}$ (mg/g)	13.51	11.24
	$K_L$ (L/mg)	0.15	0.17
	$R^2$	0.964	0.974
Freundlich	$R_L$	0.53	0.50
	$K_f$	0.34	0.33
	$n$	2.51	2.98
	$R^2$	0.959	0.996

The values of the regression coefficients indicate that the adsorption process of indigo carmine dye (IC) and Acid Orange 52 (AO52) on fly ash is described in a favorable manner by the Langmuir isotherm  $0 < R_L < 1$  and the situation as  $1/n < 1$  is more common and corresponds to a normal type L isotherm. The best fit of experimental data in the case of AO52 was obtained with the Freundlich model. The maximum absorption capacity, determined from the Langmuir isotherm, is respectively 13.51 and 11.24 (mg/g) for indigo carmine (IC) and Acid Orange 52 (AO52) respectively. Langmuir model indicate that the adsorption of dyes was made up homogenous surface and monolayer adsorption and the separation factor  $R_L$  is in the range  $0 < R_L < 1$ , showing that the adsorption of dyes on fly ash is favorable. These values confirm that fly ash have a greater capacity for adsorption of the anionic dyes.

### 3.2.4. Adsorption kinetics

In order to identify the type or the order of the kinetics of retention of the two dyes by the fly ash, three models were tested.

#### The pseudo first order kinetic

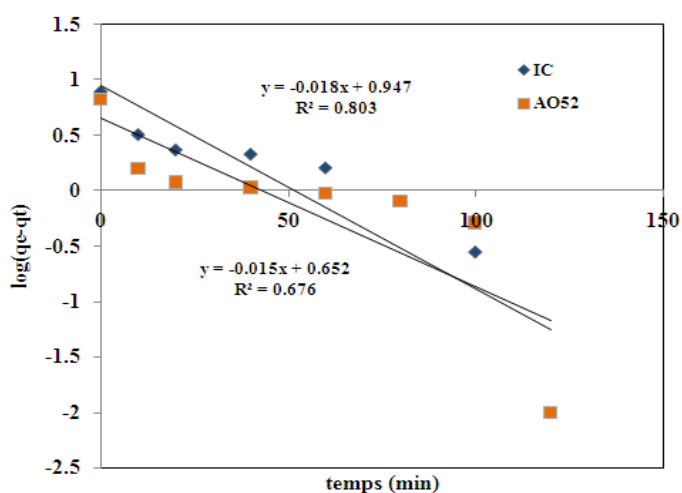


**Figure 8:** Pseudo-first-order kinetic model for adsorption of IC and AO52 on fly ash.

#### The Pseudo-second order kinetic

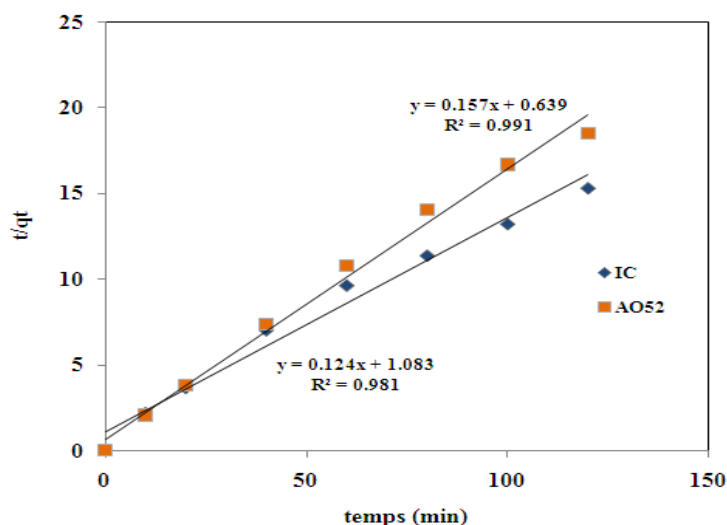


**Figure 9:** Pseudo-second-order kinetic model for adsorption of IC and AO52 on fly ash.

### Intra-particle diffusion kinetic

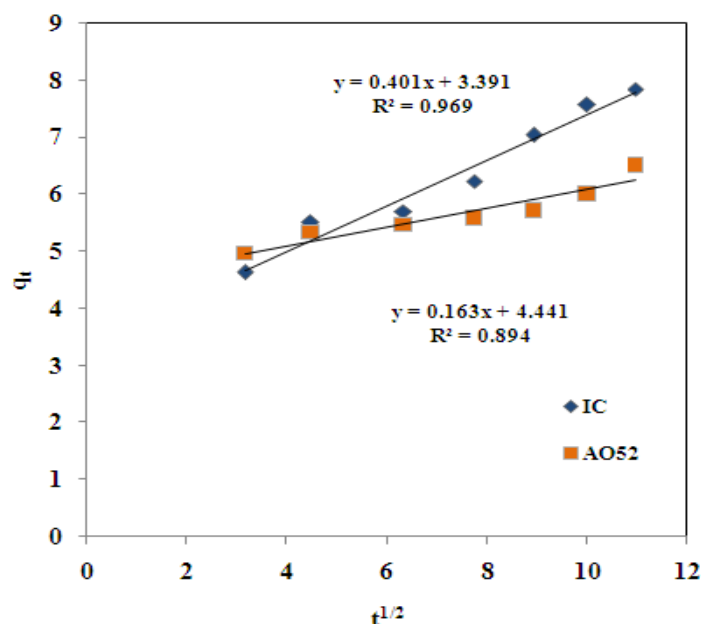


**Figure 10:** Intra-particle diffusion kinetic model for adsorption of IC and AO52 on fly ash.

The experimental data for the fly ash were fitted using the pseudo-first-order, pseudo-second-order kinetics and intraparticle diffusion models. Table 5 reports the parameters obtained using each of the models.

**Table 5:** Kinetic constants for dyes adsorption onto fly ash

	Pseudo-first-order		Pseudo-second-order		Intra-particle diffusion model	
	$k_1$ ( $\text{min}^{-1}$ )	$R^2$	$k_2$ ( $\text{g}/\text{mg}\cdot\text{min}^{-1}$ )	$R^2$	$k_{\text{int}}$ ( $\text{mg}/\text{g}\cdot\text{min}^{1/2}$ )	$R^2$
IC	<b>0.018</b>	0.803	0.039	0.991	0.401	0.969
AO 52	<b>0.015</b>	0.676	0.014	0.981	0.163	0.894

From these results, the pseudo-first-order and intra-particle diffusion models did not represent the kinetics well; meaning, their regression coefficients were lower than those obtained using the second-order kinetics model. The pseudo-second order model seems to be more adapted to describe the adsorption dynamics of the anionic dyes (IC and AO52) on the fly ash to the good correlation parameters calculated by the model with experimental data. The linearity of the plots (linear regression coefficients > 0.98) confirmed the pseudo-second-order nature of the process.

#### 3.2.5. Thermodynamic adsorption

To test the influence of the temperature of the solution on the adsorption of indigo carmine (CI) and acid orange 52 (AO52) on the fly ash, the adsorption studies were undertaken to evaluate the thermodynamic parameters at different temperatures (20, 40, 60, 80°C). From these results, the thermodynamic parameters including the change of the free energy ( $\Delta G^\circ$ ), enthalpy ( $\Delta H^\circ$ ) and entropy ( $\Delta S^\circ$ ) were used to describe the thermodynamic behavior of the adsorption of IC and AO52 onto the fly ash.

The evolution of  $\ln K_d$  versus  $1/T$  illustrated in Figure 11 allowed us to deduce the thermodynamic systems on adsorbent / adsorbate studied. It can be concluded the decrease adsorption capacity with increasing temperature and the adsorption process was found to be exothermic in nature in the case of indigo carmine and acid orange52. The free enthalpy of the system is negative and it follows a spontaneous process. Furthermore,

examination of the values of the standard enthalpy of adsorption (<40kJ/mol) displays a physical and non-specific adsorption on to the surfaces of the fly ash [46].

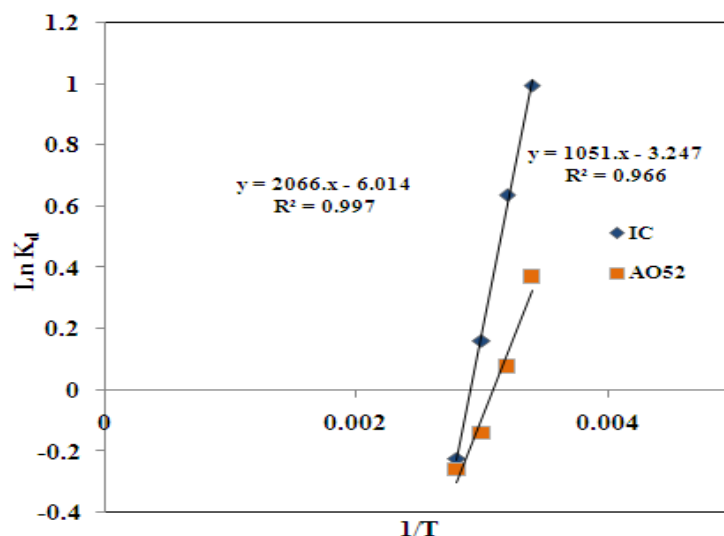


Figure 11: Plot of Ln  $K_d$  versus  $1/T$

The calculated constants were reported in Table 6.

Table 6: Thermodynamic parameters calculated for the adsorption of dyes by the fly ash

adsorbent	Adsorbate	Thermodynamic parameters					
		$\Delta H^\circ$ (KJ.mol <sup>-1</sup> )	$\Delta S^\circ$ (J.mol <sup>-1</sup> .K <sup>-1</sup> )	$\Delta G^\circ$ (J.mol <sup>-1</sup> )			
				293K	313K	333K	353K
Fly ash	IC	-17,17	-44,99	-2426,14	-1659,88	-443,86	653,3
	AO52	-8,74	-26,99	-900,91	-200,82	388,19	758,78

## Conclusion

In the present investigation, the application of fly ash was considered for the adsorption of anionic dyes in aqueous phase. The kinetic experiments suggested that the adsorption process was completed in relatively short time period, the removal of anionic dyes was influenced by solution pH. The results obtained, firstly, that the retention of the two dyes on fly ash is described by the Langmuir isotherm and corresponds to a normal type L. The kinetic data tends to fit very well in the pseudo second-order kinetics model with high correlation coefficients. The low values found for the heat of adsorption (<40 kJ/mole) mean that the anionic dyes are physically adsorbed on the fly ash surfaces. The highest percentage removal obtained for the two anionic dyes allow us to conclude that the fly ash is an excellent low cost adsorbent in the removal of anionic dyes in aqueous phase.

## References

1. Karaca S., Gurses A., Acıkyıldız M., Ejder (Korucu). M., *Microporous Mesoporous Mater.* 115(2008) 376-382.
2. Rezaee A., Masoumbeigi H., Soltani RDC., Khataee AR., Hashemiyani S., *Desalin. Water Treat.* 44(2012) 174-179.
3. Gürses A., Karaca S., Doğar C., Bayrak R., Açıkyıldız M., Yalçın M., *J. Colloid Interf. Sci.* 269 (2004) 310-314.

4. Reife A., Dyes environmental chemistry, in: Kirk-Othmer Encyclopedia of Chemical Technology, John-Wiley & Sons New York, NY, 1993.
5. Barragan B.E., Costa C., Marquez M.C., *Dyes Pigments*. 75(2007)73-81.
6. Yasin Y., Hussein M.Z., Ahmad F.H., *the Malaysian J. Analytical Sci.* 11(2007) 400-406.
7. Srinivasan S.V., Rema T., Chitra K., Sri Balakameswari K., Suthanthararajan R., Uma B., Uma Maheswari, Ravindranath E., Rajamani S., *Desalination*. 235(2009) 88-92.
8. Khadhraoui M., Trabelsi H., Ksibi M., Bouguerra S., Elleuch B., *J.Hazard Mater.* 161(2009) 974-981.
9. Pannuzo S., Rovel J.M., *L'eau, l'industrie, les nuisances*. 235(2000)123-129.
10. Bes-Pia A., Mendoza-Roca J.A., Roig-Alcover L., Iborra-Clar A., Alcaina-Miranda M.I., *Desalination*. 157 (2003) 81–86.
11. Choy Keith K.H., McKay G., Porter J.F., *Resour. Conserv. Recycl.* 27(1999) 57-71.
12. Faria P. C. C., Orfão J. J. M., M. F. R. Pereira., *Water Res.* 38(2004) 2043-2052.
13. Gomez V., Larrechi M.S., Callao M.P., *Chemosphere*. 69(2007) 1151-1158.
14. Lin S.H., *J.Chem. Tech. Biotechnol.* 57(1993) 387-391.
15. McKay G., Porter J.F., Prasad G.R., *Water Air Soil Pollut.* 114 (1999) 423–438.
16. Faria P. C. C., Orfão J. J. M., Pereira M. F. R., *Water Res.* 38 (2004)2043-2052.
17. Gomez V., Larrechi M.S., Callao M.P., *Chemosphere*. 69 (2007) 1151-1158.
18. McKay ., Ramprasad G., Mowli, *Water Res.* 21 (1987) 375-377.
19. Wang CC., Juang LC., Hsu TC., Lee CK., Lee JF., Huang FC., *J. Colloid Interf. Sci.* 273 (2004) 80–86.
20. Barka N., Assabbane A., Nounah A., Laanab L., Aïtchou Y., *Desalination*. 235 (2009) 264–275.
21. Dogan M., Karaoglu M.H., Alkan M., *J.Hazard. Mater.* 165 (2009) 1142–1151.
22. Zarezadeh-Mehrizi M., Badieli A., *Water Resour. Ind.* 5 (2014) 49–57.
23. Mane V.S., Porter Mall I.D., Srivastava V .C., *J. Environ. Manage.* 84 (2007) 390–400.
24. Janos P., Buchtova H., Ryznarova M., *Water Res.* 37 (2003) 4938–4944.
25. Eren Z., Acar F.N., *J. Hazard. Mater.* 143 (2007) 226–232.
26. Wang S., Zhu Z.H., *J. Hazard. Mater.* 126 (2005) 91–95.
27. Rachakornkij M., Ruangchuay S., Teachakulwiroj S., Songklanakarin., *J. Sci. Technol.* 26 (2004) 13–24.
28. DrKamar Shah Ariffin ,EBS 425/3 - Perindustrian Mineral. Fly ash-coal Combustion residue, *OlehDisediakan*Page 2 of 4.
29. Vasudevan D., Bruland G.L., Torrance B.S., Upchurch V.G., MacKay A.A., *Geoderma*. 151 (2009) 68–76.
30. Langmuir I., *J. Am. Chem. Soc.* 40 (1918) 1361–1403.
31. Mimanne G., Benhabib K., Benghalem A., Taleb S., *J. Mater. Environ. Sci.* 5 (2014) 1298-1307.
32. El Geundi M.S., *Adsorption Sci. Tech.* 15 (1977) 777-787.
33. Gérente C., Lee V.K.C., Le Cloirec P., McKay G., *Crit. Rev. Environ. Sci. Technol.* 37 (2007) 41–127.
34. ÖzacaM., Şengilİ.A., *J. Hazard. Mater.* 98 (2003) 211-224.
35. Febrianto J., Kosasih A.N., Sunarso J., Ju Y. Indraswati N, Ismadji S., *J. Hazard. Mater.* 162 (2009) 616–645.
36. Lagergren S., Sven K.. *Vetenskapsakad. Hand., Band.24* (1898)1–39.
37. Kumar A., Kumar S., Gupta D.V., *J. Hazard. Mater.* 147 (2007) 155-166.
38. Crini G., Peindy H.N., Gimber F., Robert C., *Separ.Purif. Technol.* 53 (2007) 97-110.
39. ÖzacarM., Sengilİ.A., *Physicochem. Eng. Aspects.* 242 (2004) 105-113.
40. Rytwo G., Ruiz-Hitzky E., *J. Thermal Analysis Calorimetry.* 71 (2003) 751-759.
41. Xu, Tan X.L., Chen C.L., Wang X.K., *J. Appl. Sci.* 41 (2008) 37-46.
42. ÖzcanA.S., ÖzcanA., *J. Colloid Interf. Sci.* 276 (2004) 39-46.
43. Bellarbi A., Monkade M., Zradba A., Laameyem A., *J. Environ. Sci. Eng.* 4 (2015) 286-294.
44. Sunil J., Kulkarni, Sonali R., Dhokpande, Dr. Jayant P. Kaware., *International J. Eng. Res. Techo.* 2 (2013) 5.
45. Sumanjit, Seema Rani, Mahajan R.K., *Arabian J. Chem.* (2012).
46. DjamelBelaid K., Kacha S., *J. Water Science.* 24 (2011) 131-144.

(2017) ; <http://www.jmaterenvirosci.com>